

Contents lists available at ScienceDirect

#### Science Bulletin

journal homepage: www.elsevier.com/locate/scib



#### Article

## Chromite-induced magnesium isotope fractionation during mafic magma differentiation

Ben-Xun Su <sup>a,b,c,\*</sup>, Yan Hu <sup>b</sup>, Fang-Zhen Teng <sup>b</sup>, Ke-Zhang Qin <sup>a,c</sup>, Yang Bai <sup>a,c</sup>, Patrick Asamoah Sakyi <sup>d</sup>, Dong-Mei Tang <sup>a</sup>

- <sup>a</sup> Key Laboratory of Mineral Resources, Institute of Geology and Geophysics, Chinese Academy of Sciences, Beijing 100029, China
- <sup>b</sup> Department of Earth and Space Sciences, University of Washington, Seattle, WA 98195, USA
- <sup>c</sup> University of Chinese Academy of Sciences, Beijing 100049, China
- <sup>d</sup> Department of Earth Science, University of Ghana, Legon, Accra LG 5, Ghana

#### ARTICLE INFO

# Article history: Received 7 September 2017 Received in revised form 25 October 2017 Accepted 26 October 2017 Available online 14 November 2017

Keywords:
Mg isotopes
Alaskan-type intrusion
Arc magmatism
Magma differentiation
Chromite

#### ABSTRACT

To better understand the mechanism of Mg isotopic variation in magma systems, here we report high precision Mg isotopic data of 17 bulk rock samples including dunite, clinopyroxenite, hornblendite and gabbro and 10 pairs of dunite-hosted olivine and chromite separates from the well-characterized Alaskan-type Xiadong intrusion in NW China, which formed by continuous and high degree of lithological differentiation from mafic magmas. Chromite separates have highly variable  $\delta^{26}{\rm Mg}$  values from -0.10%to 0.40%, and are consistently heavier than coexisting olivine separates (-0.39% to -0.15%). Both mineral  $\delta^{26}$ Mg values and the degrees of inter-mineral fractionation are well correlated with geochemical indicators of magma differentiation, indicating that these inter-sample and inter-mineral Mg isotope fractionations are caused by magma evolution. The  $\delta^{26} Mg$  values range from -0.20% to -0.02% in the dunite, -0.43% in the clinopyroxenite, -0.43% to -0.28% in the hornblendite, 0.18% in the chromite-bearing hornblendite, and -0.56% to -0.16% in the gabbro. The Mg isotopic variations in different types of rocks are closely related to fractional crystallization and accumulation of different proportions of oxides vs. silicates. Chromite crystallization and accumulation is the most important factor in controlling Mg isotope fractionation during the formation of the Xiadong intrusion. Compared to basaltic and granitic magmas, differentiation of the Alaskan-type intrusions occurs at a relatively high oxygen fugacity, which favors chromite crystallization and consequently significant Mg isotope fractionations at both mineral and whole-rock scales. Therefore, Mg isotope systematics can be used to trace the degree of magma differentiation and related-mineralization.

© 2017 Science China Press. Published by Elsevier B.V. and Science China Press. All rights reserved.

#### 1. Introduction

Magnesium isotopic variation has been increasingly reported in igneous rocks and was attributed to various mechanisms. Source heterogeneity is a main factor controlling Mg isotopic variations in volcanic rocks [1–6]; silicate-carbonatite liquid immiscibility and carbonatite magma differentiation can result in significant Mg isotope fractionation [7], whereas diffusive Mg-Fe exchange with melt or chromite produces large Mg isotope fractionation in olivine [8–11]. Although Mg isotope fractionation during the differentiation of granitic and basaltic magma is limited [3,12–15], magma differentiation involving chromite can potentially produce

large Mg isotope fractionation. This is because spinel/chromite usually is enriched in heavy Mg isotopes compared with coexisting silicates during mafic magma differentiation [16,17]. Differentiated igneous rocks with different proportions of oxides vs. silicates should therefore have different Mg isotopic compositions. However, studies of Mg isotope fractionation relevant to chromite crystallization are still limited as yet.

Alaskan-type mafic-ultramafic intrusions have several characteristics that make them ideal candidates for studying the Mg isotope fractionation during mafic magma differentiation. (1) They are considered to represent a series of cumulates derived from fractional crystallization of hydrous and oxidized primitive arc basalts [18–21] without significant crustal contamination [22,23]; (2) They are characterized by concentric occurrence of a dunite core zoned sequentially by wehrlite, clinopyroxenite, hornblendite and gabbro at the margin [19,24,25], and the different

<sup>\*</sup> Corresponding author.

E-mail address: subenxun@mail.igcas.ac.cn (B.-X. Su).

lithological units are composed of a relatively simple mineral assemblage of olivine, clinopyroxene and hornblende, and are usually dominated by a single mineral phase [26,27]; (3) Their mineral chemistry is usually characterized by Mg-rich olivine, Ca-rich diopsidic clinopyroxene, high Fe-Cr and low Al chromite, and calcic hornblende with a wide range in composition [19,28]; (4) Alaskan-type intrusions commonly host platinum group element (PGE) and chromite ore deposits, reflecting high temperature partial melts and large amount of chromite accumulation [29,30]; (5) Their enrichments in chromite, ilmenite and magnetite [24,30] predict substantial inter-mineral and inter-lithology Mg isotope fractionation resulting from significantly different Mg-O coordination environment in iron oxides and silicates [17].

Here, we report high-precision Mg isotopic data for a well-characterized Alaskan-type intrusion exposed in Xiadong, NW China. The results reveal significant mineral- and lithological- scale Mg isotope variations, reflecting Mg isotope fractionation during fractional crystallization, especially when chromite is involved. Our study suggests that Mg isotopes could be fractionated in highly oxidized magmas and consequently can be used to trace petrogenesis of mafic-ultramafic intrusions and related mineralization.

#### 2. Samples and methods

The petrology and geochemistry of the Xiadong Alaskan-type intrusion has been reported in literatures [31–34] and the broader geological context has been given by Qin et al. [35] and Su et al. [36]. The Xiadong intrusion contains a full spectrum of lithology of a typical Alaskan-type intrusion. It consists of dunite, hornblende clinopyroxenite, hornblendite and hornblende gabbro (Fig. 1a). All these rocks are characterized by a dominance of cumulate crystals with insignificant crystallization of inter-cumulus minerals filling the interstitial spaces (Fig. 1b-e). The dunites are made up of olivine (80%–95% in volume) and chromite (5%–20%) with accessory hornblende and clinopyroxene (<1%-2%). Chromite rhythmic layers are commonly observed in the dunite (Fig. 1b). The hornblende clinopyroxenite and hornblendite display gradual transitive or intrusive contact (Fig. 1c) and are mainly composed of clinopyroxene and hornblende with accessory magnetite and/or chromite (Fig. 1d). Hornblende gabbro is the dominant rock type in the Xiadong intrusion (Fig. 1a) and displays an equigranular texture with a mineral assemblage of plagioclase, clinopyroxene, hornblende, magnetite, ilmenite and titanite (Fig. 1e).

The geochemistry of these rocks suggests derivation of highdegree partial melting from a depleted mantle source. The bulk intrusive rocks are characterized by extremely low trace element abundances and flat REE patterns with mantle-like  $\varepsilon_{Nd}(t)$  [33]. The constituent olivine has high forsterite (Fo) numbers (92.3 to 96.6) and NiO contents (up to 0.76 wt%) [31,32]. Clinopyroxene hornblende are MgO-rich diopside and magnesiohornblende, respectively. In addition to the mafic silicates, various types of oxides are present in the Xiadong intrusion, displaying an Fe enrichment trend from Cr-Al-rich spinel to Fe-rich chromite to Cr-magnetite and ilmenite, with increasing degree of magma differentiation. The presence of abundant hornblende and oxides indicates that the parental magmas of the Xiadong intrusion are hydrous and oxidized [32,34]. This is consistent with the whole rock enrichments in large ion lithophile elements relative to high strength field elements, oceanic-trend (87Sr)<sup>86</sup>Sr)<sub>i</sub> variation and higher-than-mantle  $\delta^{18}$ O values, all of which indicates overprinting of the depleted mantle source by subduction-related materials [33].

Eighteen samples with comprehensive geochemical datasets [32,33] were selected for Mg isotope analyses in this study to cover the full range of lithology. They comprise 10 dunite, one clinopyroxenite, three hornblendite and four gabbro samples. Paired olivine and chromite separates were handpicked from the 10 dunite samples under a binocular microscope. They were cleaned with Milli-Q water for  $3\times 10$  min in an ultrasonic bath, and dried down under a heat lamp before dissolution.

Magnesium isotope analyses were carried out at the Isotope Laboratory of the University of Washington, Seattle, following the method described by Teng et al. [14,15,37]. Both whole-rock powders and mineral separates were dissolved in a combination of HF-HNO<sub>3</sub>-HCl in sealed 7-mLTeflon beakers and heated on a hot plate in a laminar flow exhaust hood. The samples were then dried and re-dissolved in 1 mol/L HNO<sub>3</sub> for chromatographic separation. Magnesium was purified on a cation exchange resin (Bio-rad AG50W-X8) in 1 mol/L HNO<sub>3</sub> media. The same column procedure was performed twice in order to effectively remove matrix elements. Magnesium isotopic ratios were measured on a Nu Plasma multi-collector inductively coupled plasma mass spectrometer. Three standards (JB-1 basalt, PCC-1 peridotite and Hawaiian seawater) were processed and analyzed with each batch of samples to assess accuracy and reproducibility. One analysis of basalt standard (IB-1) yielded  $\delta^{26}$ Mg value of -0.22%; two analyses of

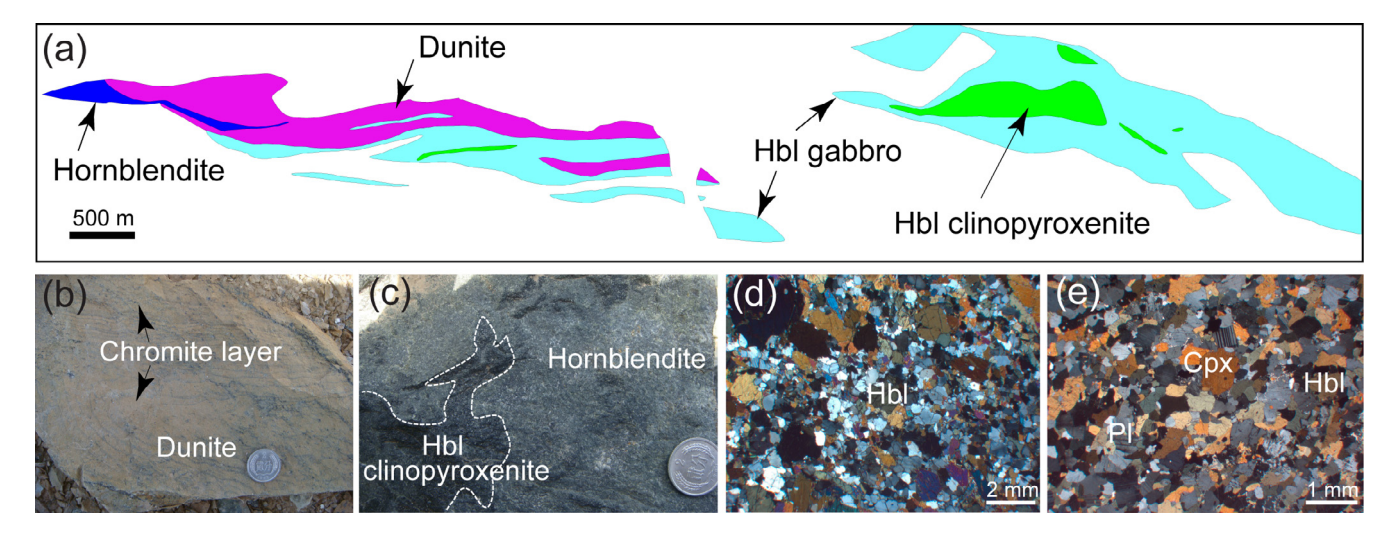


**Fig. 1.** Geological map of the Xiadong mafic-ultramafic intrusion (a) and photomicrographs of the rocks (b–e). (b) Partly bent chromite layer in dunite; (c) Intrusive relation between hornblende (Hbl) clinopyroxenite and hornblendite; (d) Adcumulate texture of hornblendite (cross polarized); (e) Typical mineral assemblage of plagioclase (Pl), clinopyroxene (Cpx) and Hbl in fresh Hbl gabbro sample (cross polarized).

peridotite standard (PCC-1) yielded an identical  $\delta^{26}$ Mg value of -0.22%; and three analyses of Hawaiian seawater standard gave  $\delta^{26}$ Mg values of -0.80%, -0.81% and -0.81%. The results of these standards agreed well with the recommended values  $(-0.276\pm0.098\%$  for JB-1,  $-0.229\pm0.041\%$  for PCC-1, and  $-0.83\pm0.09\%$  for seawater, 2SD) [37].

#### 3. Results

Magnesium isotopic data are reported in Table 1 for olivine, Table 2 for chromite, and Table 3 for bulk rock from the Xiadong intrusion. The 10 dunite samples have bulk  $\delta^{26} \rm Mg$  values of -0.20% to -0.02%, while their constitutent olivine and chromite display large Mg isotope fractionation, with chromite (-0.10% to 0.40%) being variably heavier than coexisting olivine (-0.39% to -0.15%) (Fig. 2). The single chromite-bearing hornblendite sample has the highest  $\delta^{26} \rm Mg$  value of 0.18%. On the contrary, clinopyroxenite (-0.43%), hornblendite (-0.43% and -0.28%) and gabbro samples (-0.56% to -0.16%) have light Mg isotopic compositions.

#### 4. Discussion

The Xiadong Alaskan-type intrusion displays large Mg isotopic variations at both mineral and whole-rock scales. In this section, we first examine the inter-mineral Mg isotope fractionation between chromite and olivine during mafic magma differentiation, then constrain the role of chromite crystallization in whole-rock Mg isotopic variations, and finally discuss the implications of Mg isotopes for the magma differentiation and mineralization.

#### 4.1. Large chromite-olivine Mg isotope fractionation

Based on the relative Mg-O bond strength, a sequence of  $^{26}\text{Mg}$  enrichments has been proposed: spinel/chromite > magnetite > oli vine [17]. All chromite separates analyzed here have significantly heavier Mg isotopic compositions than coexisting olivine with  $\Delta^{26}\text{Mg}_{\text{chromite-olivine}}=0.16\%$  to 0.64% (Figs. 2, 3), which is consistent with the theoretical prediction. However, the fractionation between chromite and olivine varies  $\sim\!0.5\%$  at a restricted temperature range of 965–1111 °C (Fig. 3a). This suggests that the inter-mineral fractionation is either kinetic or reflects the effect of compositional variation in the chromites on equilibrium chromite-olivine fractionation.

Kinetic fractionation induced by sub-solidus Fe-Mg interdiffusion between olivine and chromite has been well documented in studies of layered intrusions and ophiolites, during which Mg in chromite and Fe in olivine exchange with each other [11,28,38,39]. Since light isotopes diffuse faster than their heavy counterparts [40], this process will lead to higher Mg# and lower  $\delta^{26}$ Mg in olivine with a corresponding increase in  $\delta^{26}$ Mg of chromite, which agrees with the results of olivine-chromite pairs from Tibetan ophiolites [11]. This is opposite, however, to the positive correlation between Mg# and  $\delta^{26}$ Mg observed in the olivine from the Xiadong dunite (Fig. 2a), hence sub-solidus Fe-Mg exchange can be ruled out.

The large chromite-olivine fractionation thus likely reflects the effect of compositional variation in the oxides. Theoretical calculation suggests the degree of equilibrium isotope fractionation between spinel/chromite and olivine strongly depends on the octahedral ion composition (i.e.,  $B^{3+}$ ) in spinel/chromite ( $A^{2+}B_2^{3+}O_4^{2-}$ ) [17]. For example, at 1000 °C, the magnitude of inter-mineral fractionation varies from 0.6% for spinel (MgAl<sub>2</sub>O<sub>4</sub>) to 0.2% for magnesiochromite (MgCr<sub>2</sub>O<sub>4</sub>), to 0.1% for magnesioferrite (MgFe<sub>2</sub>O<sub>4</sub>) [17]. Natural chromite that contains various proportions of these different endmembers will therefore be heavier than coexisting olivine by 0.1% to 0.6%. The fractionation of the 10 olivinechromite pairs from the Xiadong dunite varies from 0.16% to 0.64% (Fig. 3a), which largely falls in the range of theoretically calculated fractionations between olivine and different spinel endmembers. Compared to the limited compositional variations in the olivine (e.g., Mg# and  $\delta^{26}$ Mg in Table 1), the chromite in the Xiadong dunite is highly variable with respect to TiO2, NiO, and  $Fe^{3+}$  + Al + Cr cation, as well as  $Fe^{3+}/(Fe^{3+} + Al + Cr)$  ratio (Table 2). These chemical parameters are negatively or positively correlated with the  $\delta^{26} \rm Mg$  values of the chromite and  $\Delta^{26} \rm Mg_{chromite-olivine}$  values (Figs. 2 and 3). This suggests that the change in chromite composition significantly affects the inter-mineral fractionation. Meanwhile, it has been well established that the composition of chromite in magma systems is mainly controlled by magma differentiation [38.41–43]. Therefore, crystallization of chromite and its compositional change during magma evolution are responsible for the large chromite-olivine Mg isotope fractionation.

The compositional variations of olivine and chromite (e.g., Fo and NiO in olivine,  $TiO_2$  and NiO in chromite) are sensitive indicators of magma differentiation [38,43]. With differentiation of the whole magma system from mafic to felsic, the

**Table 1**Mg isotopic compositions and selected geochemical parameters of olivine (OI) in the dunite from the Xiadong Alaskan-type intrusion.

	_	-			_				
Sample	Rock type	Mineral	δ <sup>26</sup> Mg (‰)	2SD <sup>a</sup>	$\delta^{25}$ Mg (‰)	2SD	FeO <sup>b</sup> (wt.%)	NiO <sup>b</sup> (wt.%)	Mg# <sup>b</sup>
09XDTC1-15	Dunite	Ol	-0.29	0.07	-0.15	0.05	5.60	0.35	94.5
09XDTC1-35	Dunite	Ol	-0.31	0.07	-0.18	0.07	5.00	0.36	95.0
09XDTC1-16	Dunite	Ol	-0.24	0.07	-0.12	0.03	4.98	0.34	95.1
Repeat <sup>c</sup>	Dunite	Ol	-0.27	0.05	-0.13	0.06			
Repeat <sup>c</sup>	Dunite	Ol	-0.23	0.07	-0.11	0.04			
Repeat <sup>c</sup>	Dunite	Ol	-0.27	0.07	-0.11	0.07			
09XD-1	Dunite	Ol	-0.39	0.10	-0.19	0.02	4.85	0.27	95.2
Repeat <sup>c</sup>	Dunite	Ol	-0.34	0.06	-0.16	0.06			
Repeat <sup>c</sup>	Dunite	Ol	-0.37	0.06	-0.19	0.05			
09XDTC1-28	Dunite	Ol	-0.18	0.09	-0.08	0.04	4.36	0.48	95.7
09XDTC1-36	Dunite	Ol	-0.32	0.07	-0.20	0.07	4.15	0.32	95.9
09XDTC1-29	Dunite	Ol	-0.24	0.07	-0.12	0.07	4.04	0.44	96.0
09XDTC1-24	Dunite	Ol	-0.25	0.07	-0.14	0.07	3.64	0.29	96.4
09XDTC1-25	Dunite	Ol	-0.15	0.07	-0.09	0.07	3.59	0.32	96.4
09XDTC1-32	Dunite	Ol	-0.23	0.11	-0.12	0.06	3.55	0.23	96.5

#### Note:

 $<sup>^{</sup>a}$  2SD = two times the standard deviation of the population of n (n > 20) repeat measurements of the standards during an analytical session.

<sup>&</sup>lt;sup>b</sup> Data are from Su et al. [32]; Mg# = Mg/(Mg + Fe<sup>2+</sup>)  $\times$  100.

<sup>&</sup>lt;sup>c</sup> Repeat = repeat dissolution and column chemistry of individual samples.

**Table 2**Mg isotopic compositions and selected geochemical parameters of chromite (Chr) in the dunite from the Xiadong Alaskan-type intrusion.

Sample	Rock type	Mineral	δ <sup>26</sup> Mg (‰)	2SD	δ <sup>25</sup> Mg (‰)	2SD	TiO <sub>2</sub> <sup>a</sup> (wt.%)	NiO <sup>a</sup> (wt.%)	$100 \times Fe^{3+}/(Fe^{3+} + Al + Cr)^{3}$
09XDTC1-15	Dunite	Chr	0.26	0.07	0.17	0.05	0.14	0.56	81.6
09XDTC1-35	Dunite	Chr	0.09	0.07	0.06	0.05	0.12	0.72	98.7
09XDTC1-16	Dunite	Chr	0.40	0.07	0.22	0.05	0.09	0.68	85.7
09XD-1	Dunite	Chr	0.10	0.07	0.04	0.05	0.22	0.81	79.8
09XDTC1-28	Dunite	Chr	0.16	0.07	0.09	0.05	0.27	1.02	81.7
09XDTC1-36	Dunite	Chr	0.26	0.07	0.11	0.05	0.18	0.73	78.9
09XDTC1-29	Dunite	Chr	0.05	0.07	0.02	0.05	0.12	0.86	89.1
09XDTC1-24	Dunite	Chr	-0.10	0.07	-0.07	0.05	0.00	1.01	83.9
09XDTC1-25	Dunite	Chr	0.01	0.07	0.02	0.05	0.05	0.96	92.9
09XDTC1-32	Dunite	Chr	0.18	0.07	0.12	0.05	0.16	0.64	69.7

Note:

**Table 3**Mg isotopic compositions and selected geochemical parameters of intrusive rocks from the Xiadong Alaskan-type intrusion.

Sample	Rock type	δ <sup>26</sup> Mg (‰)	2SD	$\delta^{25}$ Mg (‰)	2SD	Fe <sub>2</sub> O <sub>3</sub> <sup>a</sup> (wt.%)	FeO <sup>a</sup> (wt.%)	Mg#ª	Li <sup>a</sup> (ppm)	Sc <sup>a</sup> (ppm)	∑PGE <sup>a</sup> (ppb)
09XDTC1-15	Dunite	-0.12	0.05	-0.04	0.04	5.72	2.77	90.5	5.82	4.18	8.87
09XDTC1-35	Dunite	-0.04	0.05	-0.04	0.04	5.21	1.97	91.5			111.9
09XDTC1-16	Dunite	-0.11	0.05	-0.01	0.04						
Repeat <sup>b</sup>		-0.08	0.07	-0.03	0.06						
09XD-1						5.67	3.15	90.1	5.04	6.43	
09XDTC1-28	Dunite	-0.02	0.05	0.01	0.04	3.76	2.34	92.7	5.78	3.65	8.69
09XDTC1-36	Dunite	-0.19	0.05	-0.12	0.04	5.39	2.90	91.2	4.65	2.97	33.6
09XDTC1-29	Dunite	-0.19	0.05	-0.07	0.04	5.07	2.92	90.8			13.9
09XDTC1-24	Dunite	-0.15	0.05	-0.07	0.04	5.34	1.91	91.9			9.52
09XDTC1-25	Dunite	-0.09	0.05	-0.04	0.04	9.08	3.22	86.5	5.83	5.77	11.6
09XDTC1-32	Dunite	-0.20	0.05	-0.12	0.04	5.07	2.86	91.4	6.99	4.32	9.78
09XDTC1-10	Hbl Cpxt	-0.43	0.07	-0.26	0.06	3.65	3.25	88.3	9.58	19.6	3.41
09XDTC1-21	Hblt	-0.28	0.07	-0.12	0.06	6.66	6.11	56.9	19.9	33.1	2.08
09XDTC1-37	Hblt (Chr-bearing)	0.18	0.07	0.14	0.05	11.1	5.25	57.7	8.09	25.9	0.70
Repeat <sup>b</sup>		0.15	0.06	0.08	0.08						
Repeat <sup>b</sup>		0.13	0.06	0.07	0.05						
Repeat <sup>b</sup>		0.20	0.07	0.11	0.07						
09XDTC1-44	Hblt	-0.43	0.1	-0.21	0.08	4.25	10.3	58.5	16.2	38.9	0.38
09XDTC1-8	Hbl Gbr	-0.56	0.07	-0.30	0.06	2.97	6.59	66.6	19.2	28.2	0.54
09XDTC1-12	Hbl Gbr	-0.16	0.07	-0.08	0.06	8.07	4.91	44.5	14.1	23.4	0.41
09XDTC1-22	Hbl Gbr	-0.21	0.07	-0.11	0.06	4.97	4.93	56.2	10.6	25.9	1.63
XDE2	Hbl Gbr	-0.20	0.05	-0.10	0.04	0.25	0.77	93.5	7.22	17.7	6.98

Chr, chromite; Cpxt, clinopyroxenite; Gbr, gabbro; Hbl, hornblende; Hblt, hornblendite. *Note*:

Mg# (Mg/(Mg + Fe)) in both olivine and chromite and the  $Fe^{3+}/(Fe^{3+} + Al + Cr)$  ratio in chromite decrease as Fe is increasingly incorporated into olivine, while less Mg and more Al enter chromite, causing a significant increase of the FeO<sub>olivine</sub>/FeO<sub>chromite</sub> ratio [38,41]. The narrow Mg# range (96.5–94.5; Table 1) of the studied olivine reflects the limited differentiation of the magma during the dunite formation. Nonetheless, there is a positive correlation between olivine  $\delta^{26}$ Mg value and Mg# number (Fig. 2a). Meanwhile, a more prominent and complementary negative correlation has been observed for the relatively MgO-poor chromite (Fig. 2a). Consistent  $\delta^{26}$ Mg variation trends with NiO, TiO<sub>2</sub> and FeO<sub>olivine</sub>/FeO<sub>chromite</sub> ratio have also been found in chromite (Fig. 2b-f). Likewise, the bulk dunite  $\delta^{26}$ Mg values are also correlated with magma differentiation indices, such as wholerock Mg#, NiO content in olivine and  $Fe^{3+}/(Fe^{3+} + Al + Cr)$  ratio in chromite, although with a shallower slope (Fig. 2 g, h). These correlations suggest that magma differentiation could induce significant inter-sample fractionations in each constituent phase, and to a lesser degree, consistent variation trends at bulk-rock scale. The magnitude of Mg isotope fractionation between chromite and olivine seems to be also controlled by the degree of magma evolution, as evidenced by the consistent  $\Delta^{26} \text{Mg}_{\text{chromite-olivine}}$  variation trends with magma differentiation indices, such as the amounts of trivalent cation, particularly Fe<sup>3+</sup> and NiO contents in chromite and Mg# in olivine (Fig. 3b, c, d).

### 4.2. Whole-rock Mg isotopic variation caused by chromite crystallization

The large Mg isotopic variation among different types of cumulates reflects the large Mg isotope fractionation between oxides and silicates. These cumulative dunite, clinopyroxenite and horn-blendite were formed by sequential crystallization of olivine  $\rightarrow$  clin opyroxene  $\rightarrow$  hornblende [32]. Since these silicate phases all have similar octahedral coordination site for Mg, they generally possess a mantle-like Mg isotopic composition (e.g., -0.31% to -0.14% in hornblende, [13]). Therefore, crystallization of these minerals was not responsible for the observed large inter-lithology variation in  $\delta^{26}$ Mg. Instead, various types of oxides (e.g., chromite, magnetite and ilmenite) crystallized and accumulated during the formation

<sup>&</sup>lt;sup>a</sup> Data are from Su et al. [32].

<sup>&</sup>lt;sup>a</sup> Data are from Su et al. [33].

b Repeat = repeat dissolution and column chemistry of individual samples.

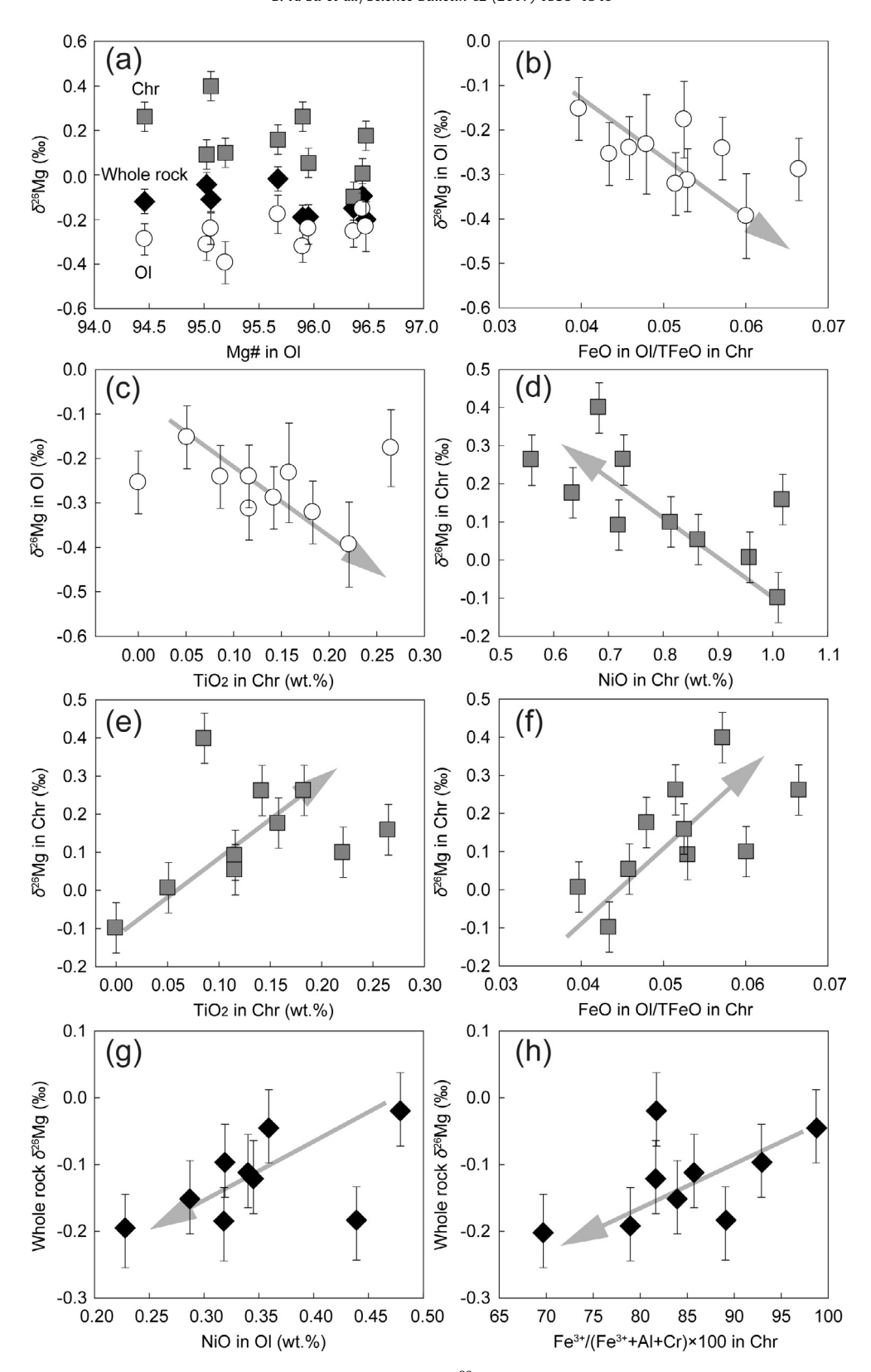


**Fig. 2.** Plots of  $\delta^{26}$ Mg in chromite, olivine and whole rock vs. Mg# in olivine (a), olivine  $\delta^{26}$ Mg vs. FeO ratio of olivine against chromite (b) and TiO<sub>2</sub> in chromite (c), chromite  $\delta^{26}$ Mg vs. NiO (d) and TiO<sub>2</sub> (e) in chromite, and FeO ratio of olivine against chromite (f), whole rock  $\delta^{26}$ Mg vs. NiO in olivine (g) and Fe<sup>3+</sup>/(Fe<sup>3+</sup> + Al + Cr)×100 in chromite (h) for Xiadong Alaskan-type intrusion. Gray arrow represents magma differentiation trend. Ol, olivine; Chr, chromite.

of the Xiadong intrusion [32]. Crystallization of these oxide species with different chemical compositions during magma differentiation can lead to large Mg isotopic variation in the bulk rock Mg isotopic composition.

Chromite is the earliest crystallized phase during mafic magma evolution and occurs as the main accessory mineral phase in the Xiadong intrusive rocks. Its modal content is particularly high, up to 5%–20% in the dunite, whereas other rock types contain sparse

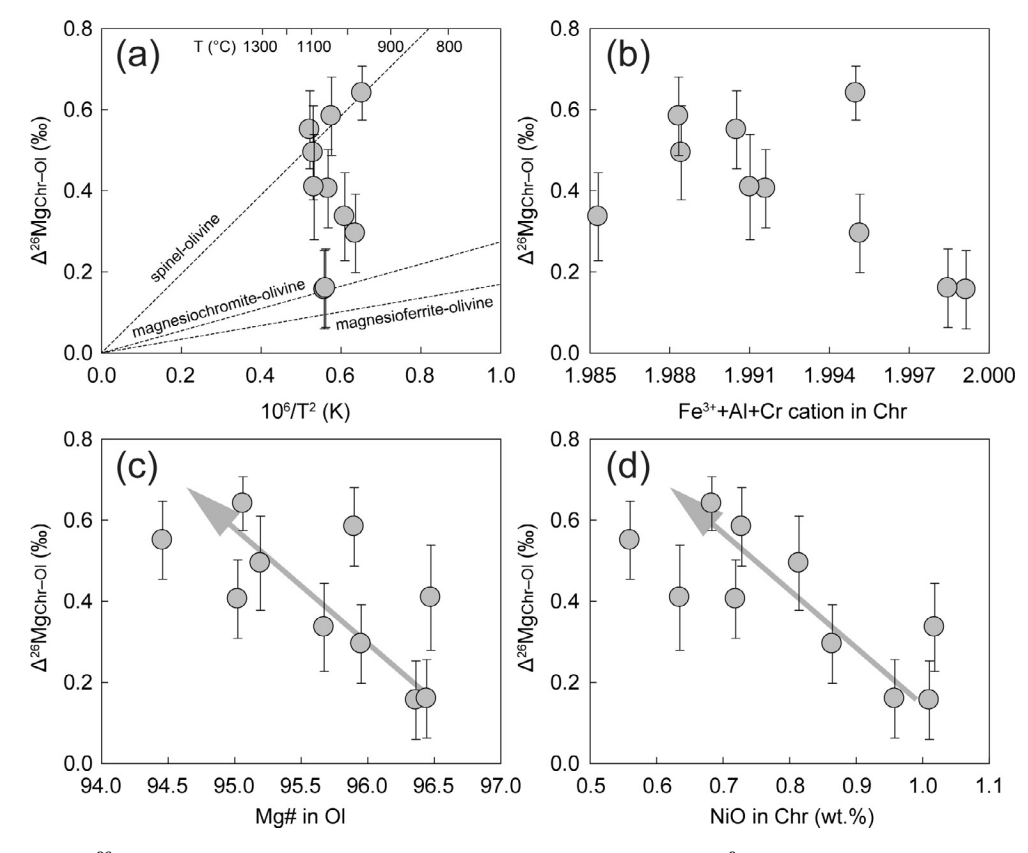


Fig. 3. Correlation diagrams of  $\Delta^{26}$ Mg<sub>Chr-Ol</sub> vs. temperature with comparison with theoretical predictions (a), Fe<sup>3+</sup> + Al + Cr cation in chromite (b; after Schauble [17]), Mg# in olivine (c), and NiO in chromite (d) for the Xiadong Alaskan-type intrusion. Gray arrow represents magma differentiation trend.

or no chromite [32]. The modal variation of chromite can account for the higher  $\delta^{26}$ Mg values in the dunite compared to other rocks (Fig. 4). The negative correlation between chromite  $Fe^{3+}/(Fe^{3+} + Al + Cr)$  ratio and dunite  $\delta^{26}Mg$  value (Fig. 2 h) suggests that Mg isotopic variation in the dunite mainly resulted from the varying chromite content. Furthermore, the anomalously high  $\delta^{26}$ Mg value (Fig. 4) in one of the hornblendite samples is consistent with its high abundance of chromite. The significant decreases in whole rock Fe<sup>3+</sup>/∑Fe ratio and Cr concentration from dunite to gabbro (Fig. 4d, e) also indicate crystallization and accumulation of different proportions of oxides vs. silicates during magma evolution. The low and anomalously high  $\delta^{26} \rm Mg$  values in the more differentiated cumulates may be caused by fractionation and accumulation of ilmenite, respectively (Fig. 4f), which has been invoked to explain the isotopically light high-Ti lunar basalts [44,45].

#### 4.3. Implications

The significant inter-lithology Mg isotopic variation observed in the Xiadong Alaskan-type intrusion relative to the limited fractionation in high-temperature magma systems reported in previous studies [12–14] is noteworthy. While source heterogeneity resulting from crustal recycling is the main cause for generating Mg isotopic variation in basalts and granites, fractional crystallization generally has insignificant effect on changing the Mg isotopic composition of evolving magmas [13,15]. This is because differentiation processes in granitic magmas are mainly associated with compositional change in Mg-poor feldspars, while the mafic minerals, which control the Mg budget, all have similar Mg isotopic compositions [13]. During basaltic differentiation, crystallization of olivine, which has a typical mantle-like  $\delta^{26}$ Mg [8,9], will have

negligible effect on the  $\delta^{26}$ Mg of the residual magmas, based on mass balance calculations. This can explain the lack of Mg isotope fractionation in basaltic lavas that have undergone various degrees of olivine crystallization [3,14,15]. On the other hand, chromite crystallization and accumulation, if occurred during magma ascent, would lower the  $\delta^{26}$ Mg value of the evolved magma, and thus, might be an alternative explanation for the anomalously light Mg isotopic compositions of the continental basalts from East Asia [1,2,4,5] (Fig. 4 g). As a consequence, effects of chromite crystallization and accumulation should be firstly evaluated before using Mg isotopes to trace magma sources and crustal recycling.

Whole rock Li and Sc concentrations are sensitive to differentiation of basaltic magmas [46,47] and display consistent variation trends with  $\delta^{26}$ Mg values for the Xiadong intrusion (Fig. 4a-c). With increasing degree of differentiation, the bulk rock  $\delta^{26}$ Mg varies from mantle-like values in the dunite to lower values in the clinopyroxenite, hornblendite and gabbro (Fig. 4a, b) with an accompanied significant decrease in chromite modal abundance. Therefore, the inter-lithology variation of the whole rock  $\delta^{26}$ Mg may reflect the composition-dependent variation of oxide  $\delta^{26}$ Mg with increasing degree of magma differentiation. As chromite mineralization is commonly associated with PGE enrichment [48], the consistent correlations of PGE and Cr concentrations with  $\delta^{26}$ Mg (Fig. 4c, e) further substantiate that PGE segregation is mainly controlled by chromite crystallization. Thus, Mg isotopic compositions of mafic-ultramafic intrusions serve as an indicator of the degree of magma differentiation and the level of oxide accumulation, which can also be used as a guide for Fe, Cr and PGE mining. In this regard, the advantage of Mg isotope systematics, comparing to other tracers, is its relative immunity to silicate mineral fractionation and crustal assimilation during magma differentiation as crustal materials contain significantly lower Mg than mafic magmas [49].

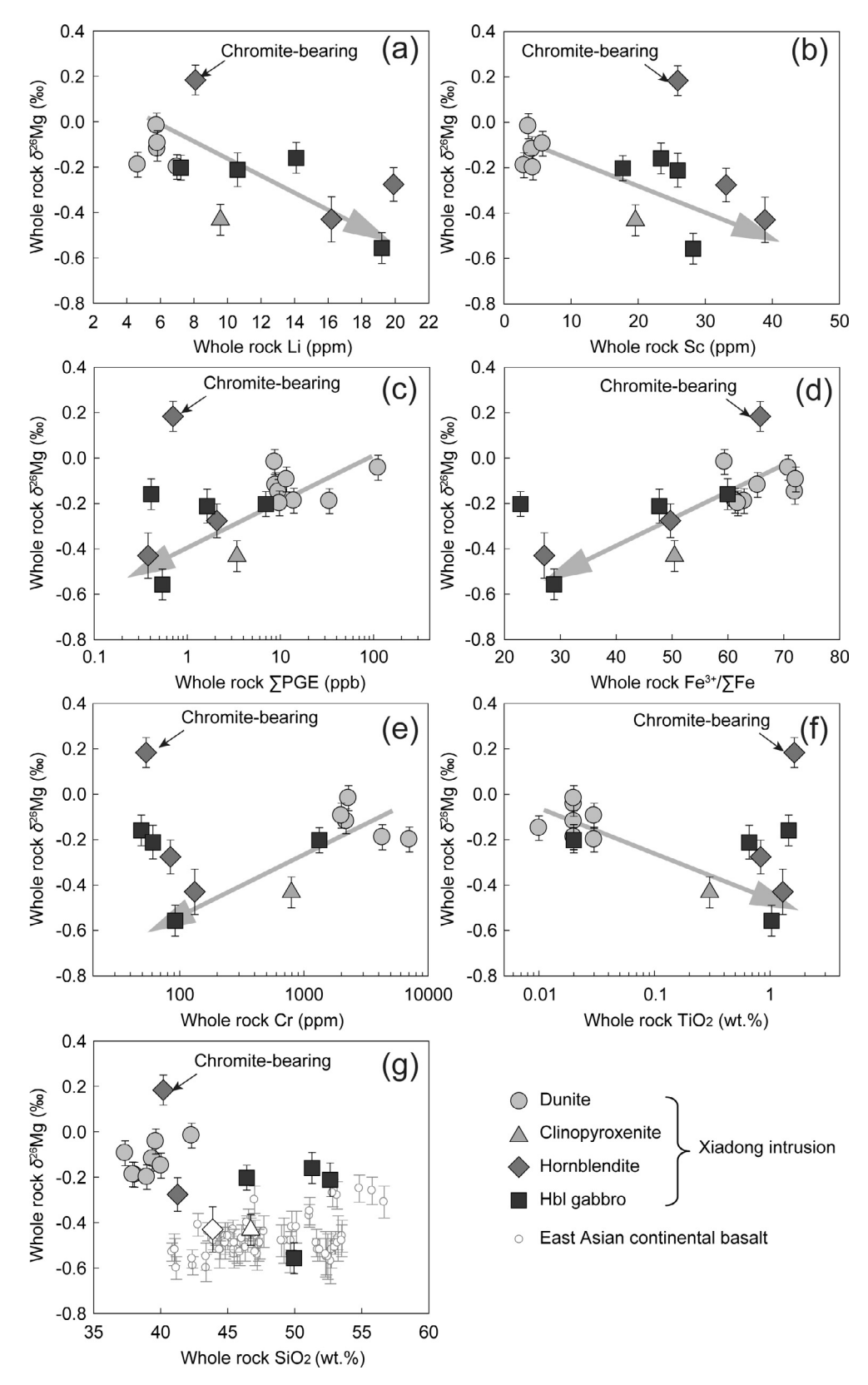


**Fig. 4.** Correlation diagrams of whole rock  $\delta^{26}$ Mg with whole rock Li (a), Sc (b),  $\sum$ PGE (c), Fe<sup>3+</sup>/ $\sum$ Fe (d), Cr (e), TiO<sub>2</sub> (f) and SiO<sub>2</sub> (g) for the Xiadong Alaskan-type intrusion. Literature data of East Asian continental basalts [1, 2, 4, 5] were plotted for comparison in Fig. 4e. Gray arrow represents magma differentiation trend.

#### 5. Conclusions

The Xiadong Alaskan-type intrusion displays considerable Mg isotopic variations at both mineral and whole-rock scales. The large chromite-olivine fractionation reflects the effect of compositional variation in chromite, while the wide Mg isotopic variation among different types of cumulates resulted from the large Mg isotope fractionation between oxides and silicate minerals. Thus, chromite crystallization and accumulation may play a crucial role in Mg isotope fractionation during the formation of the Alaskan-type intrusions. As chromite composition is mainly controlled by magma differentiation, Mg isotope systematics can be used as an indicator of oxide accumulation in magmas at depth, and also as a guide for the exploration and mining of Fe, Cr and PGE in mafic-ultramafic intrusions.

#### **Conflict of interest**

The authors declare that they have no conflict of interest.

#### Acknowledgments

Constructive comments from Xiaowei Li and two anonymous reviewers, as well as the editor, are greatly appreciated. This work was financially supported by the National Key R&D Program of China (2017YF0601204), National Natural Science Foundation of China (41522203), and National Science Foundation of United States (EAR-1747706).

#### Appendix A. Supplementary data

Supplementary data associated with this article can be found, in the online version, at https://doi.org/10.1016/j.scib.2017.11.001.

#### References

- [1] Yang W, Teng FZ, Zhang HF, et al. Magnesium isotopic systematics of continental basalts from the North China Craton: implications for tracing subducted carbonate in the mantle. Chem Geol 2012;328:185–94.
- [2] Huang J, Li SG, Xiao Y, et al. Origin of low  $\delta^{26}$ Mg Cenozoic basalts from South China Block and their geodynamic implications. Geochim Cosmochim Acta 2015;164:298–317.
- [3] Teng FZ, Hu Y, Chauvel C. Magnesium isotope geochemistry in arc volcanism. Proc Natl Acad Sci USA 2016;113:7082–7.
- [4] Tian HC, Yang W, Li SG, et al. Origin of low  $\delta^{26}$ Mg basalts with EM-I component: evidence for interaction between enriched lithosphere and carbonated asthenosphere. Geochim Cosmochim Acta 2016;188:93–105.
- [5] Su BX, Hu Y, Teng FZ, et al. Magnesium isotope constraints on subduction contribution to Mesozoic and Cenozoic East Asian continental basalts. Chem Geol 2017:466:116–22.
- [6] Sun Y, Teng FZ, Ying JF, et al. Magnesium isotopic evidence for ancient subducted oceanic crust in LOMU-like potassium-rich volcanic rocks. J Geophys Res: Solid Earth 2017:122. https://doi.org/10.1002/2017JB014560.
- [7] Li WY, Teng FZ, Halama R, et al. Magnesium isotope fractionation during carbonatite magmatism at Oldoinyo Lengai, Tanzania. Earth Planet Sci Lett 2016:444:26–33.
- [8] Teng FZ, Dauphas N, Helz RT, et al. Diffusion-driven magnesium and iron isotope fractionation in Hawaiian olivine. Earth Planet Sci Lett 2011;308:317–24.
- [9] Sio CKI, Dauphas N, Teng FZ, et al. Discerning crystal growth from diffusion profiles in zoned olivine by in situ Mg–Fe isotopic analyses. Geochim Cosmochim Acta 2013;123:302–21.
- [10] Oeser M, Dohmen R, Horn I, et al. Processes and time scales of magmatic evolution as revealed by Fe-Mg chemical and isotopic zoning in natural olivines. Geochim Cosmochim Acta 2015;154:130–50.
- [11] Xiao Y, Teng FZ, Su BX, et al. Iron and magnesium isotopic constraints on the origin of chemical heterogeneity in podiform chromitite from the Luobusa ophiolite, Tibet. Geochem Geophys Geosyst 2016;17:940–53.
- [12] Dauphas N, Teng FZ, Arndt NT. Magnesium and iron isotopes in 2.7 Ga Alexo komatiites: mantle signatures, no evidence for Soret diffusion, and identification of diffusive transport in zoned olivine. Geochim Cosmochim Acta 2010;74:3274–91.

- [13] Liu SA, Teng FZ, He Y, et al. Investigation of magnesium isotope fractionation during granite differentiation: implication for Mg isotopic composition of the continental crust. Earth Planet Sci Lett 2010;297:646–54.
- [14] Teng FZ, Li WY, Ke S, et al. Magnesium isotopic composition of the Earth and chondrites. Geochim Cosmochim Acta 2010;74:4150–66.
- [15] Teng FZ, Wadhwa M, Helz RT. Investigation of magnesium isotope fractionation during basalt differentiation: implications for a chondritic composition of the terrestrial mantle. Earth Planet Sci Lett 2007;261:84–92.
- [16] Liu SA, Teng FZ, Yang W, et al. High-temperature inter-mineral magnesium isotope fractionation in mantle xenoliths from the North China Craton. Earth Planet Sci Lett 2011;308:131–40.
- [17] Schauble E. First-principles estimates of equilibrium magnesium isotope fractionation in silicate, oxide, carbonate and hexaaquamagnesium (2+) crystals. Geochim Cosmochim Acta 2011;75:844–69.
- [18] Taylor HP. The zoned ultramafic complexes of southeastern Alaska. In: Wyllie PJ, editor. Ultramafic and related rocks. New York: Wiley Inc; 1967. p. 97–121.
- [19] Irvine TN. Petrology of the Duke Island ultramafic complex southern Alaska. Geological Society of American Memoir 1974;138:1–244.
- [20] Debari SM, Coleman RG. Examination of the deep levels of an island arc: evidence from the Tonsina ultramafic-mafic assemblage, Tonsina, Alaska. | Geophys Res 1989;94:4373–91.
- [21] Brugmann GE, Reischmann T, Naldrett AJ, et al. Roots of an Archean volcanic arc complex: the Lac des Iles area in Ontario, Canada. Precambrian Res 1997:81:223–39.
- [22] Sha LK. Genesis of zoned hydrous ultramafic-mafic silicic intrusive complexes: an MHFC hypothesis. Earth Sci Rev 1995;39:59–90.
- [23] Farahat ES, Helmy HM. Abu Hamamid Neoproterozoic Alaskan-type complex, south Eastern Desert, Egypt. J Afr Earth Sci 2006;45:187–97.
- [24] Himmelberg GR, Loney RA. Characteristics and petrogenesis of Alaskan-type ultramafic-mafic intrusions, Southeastern Alaska. US Geological Survey: Professional Papers; 1995. p. 1–47.
- [25] Su BX, Qin KZ, Santosh M, et al. The Early Permian mafic-ultramafic complexes in the Beishan Terrane, NW China: Alaskan-type intrusives or rift cumulates? J Asian Earth Sci 2013;66:175–87.
- [26] Thakurta J, Ripley EM, Li CS. Geochemical constraints on the origin of sulfide mineralization in the Duke Island complex, southeastern Alaska. Geochem Geophys Geosyst 2008;9:Q07003.
- [27] Ripley EM. Magmatic sulfide mineralization in Alaskan-type complexes. In: Li CS, Ripley EM, editors. New developments in magmatic Ni-Cu and PGE deposits. p. 219–28.
- [28] Bai Y, Su BX, Chen C, et al. Base metal mineral segregation and Fe-Mg exchange inducing extreme compositions of olivine and chromite from the Xiadong Alaskan-type complex in the southern part of the Central Asian Orogenic Belt. Ore Geol Rev 2017. https://doi.org/10.1016/j.oregeorev.2017.01.023.
- [29] Hattori K, Cabri LJ. Origin of platinum-group-mineral nuggets inferred from an osmium-isotope study. Can Mineral 1992;30:289–301.
- [30] Johan Z. Alaskan-type complexes and their platinum-group element mineralization. In: Cabri LJ, editor. Geology, Geochemistry, Mineralogy and Mineral Beneficiation of Platinum-group Elements. Canadian Institute of Mining, Metallurgy and Petroleum; 2002. p. 669–719.
- [31] Sun H, Qin KZ, Su BX, et al. Discovery of komatiitic ultramafic intrusion in Mid-Tianshan terrain: Xiadong intrusion, Xinjiang. Acta Petrol Sin 2009;25:738–48 (in Chinese).
- [32] Su BX, Qin KZ, Sakyi PA, et al. Occurrence of an alaskan-type complex in the Middle Tianshan Massif, Central Asian Orogenic Belt: inferences from petrological and mineralogical studies. Int Geol Rev 2012;54:249–69.
- [33] Su BX, Qin KZ, Zhou MF, et al. Petrological, geochemical and geochronological constraints on the origin of the Xiadong Ural-Alaskan type complex in NW China and tectonic implication for the evolution of southern Central Asian Orogenic Belt. Lithus 2014:200–201:226–40
- [34] Su BX, Chen C, Bai Y, et al. Lithium isotopic composition of Alaskan-type intrusion and its implication. Lithos 2017;286–287:363–8.
- [35] Qin KZ, Su BX, Sakyi PA, et al. SIMS Zircon U-Pb geochronology and Sr-Nd isotopes of Ni-Cu bearing mafic-ultramafic intrusions in Eastern Tianshan and Beishan in correlation with flood basalts in Tarim Basin (NW China): constraints on a ca. 280 Ma mantle plume. Am J Sci 2011;311:237–60.
- [36] Su BX, Qin KZ, Sakyi PA, et al. U-Pb ages and Hf-o isotopes of zircons from Late Paleozoic mafic-ultramafic units in southern Central Asian Orogenic Belt: tectonic implications and evidence for an Early-Permian mantle plume. Gondwana Res 2011;20:516–31.
- [37] Teng FZ, Li WY, Ke S, et al. Magnesium isotopic compositions of international geological reference materials. Geostand Geoanal Res 2015;39:329–39.
- [38] Jackson ED. Chemical variation in coexisting chromite and olivine in chromitite zones of Stillwater complex. Econ Geol Monogr 1969;4:41–71.
- [39] Melcher F, Grum W, Simon G, et al. Petrogenesis of the ophiolitic giant chromite deposits of Kempirsai, Kazakhstan: a study of solid and fluid inclusions in chromite. J Petrol 1997;38:1419–58.
- [40] Richter FM, Watson EB, Mendybaev RA, et al. Magnesium isotope fractionation in silicate melts by chemical and thermal diffusion. Geochim Cosmochim Acta 2008;72:206–20.
- [41] Roeder PL, Campbell IH, Jamieson HE. Re-evaluation of the olivine-spinel geothermometer. Contrib Mineral Petrol 1979;68:325–34.

- [42] Sickafus KE, Wills JM, Grimes JW. Structure of spinel. J Am Ceramic Soci 1999;82:3279–92.
- [43] Kamenetsky VS, Crawford AJ, Meffre S. Factors controlling chemistry of magmatic spinel: an empirical study of associated olivine, Cr-spinel and melt inclusions from primitive rocks. J Petrol 2001;42:655–71.
- [44] Wiechert U, Halliday AN. Non-chondritic magnesium and the origins of the inner terrestrial planets. Earth Planet Sci Lett 2007;256: 360–71.
- [45] Sedaghatpour F, Teng FZ, Liu Y, et al. Magnesium isotopic composition of the Moon. Geochim Cosmochim Acta 2013;120:1–16.
- [46] Winchester JA, Floyd PA. Geochemical discrimination of different magma series and their differentiation products using immobile elements. Chem Geol 1977;20:325–43.
- [47] Teng FZ, Rudnick RL, McDonough WF. Lithium isotopic systematics of A-type granites and theirmafic enclaves: further constraints on the Li isotopic composition of the continental crust. Chem Geol 2009;262:370–9.
- [48] Crocket JH. Platinum-group elements in basalts from Maui, Hawaii: low abundances in alkali basalts. Can Mineral 2002;40:595–609.
- [49] Teng FZ. Magnesium isotope geochemistry. Rev Mineral Geochem 2017;82:219–87.